Synthesis of SiO_2-Aerogel Inverse Opals in Supercritical Carbon Dioxide

Albertina Cabañas,*,† Eduardo Enciso,† M. Carmen Carbajo,‡ María J. Torralvo,‡ Concepción Pando,† and Juan Antonio R. Renuncio†

Departamento de Química−Física I y Departamento de Química Inorgánica I, Universidad Complutense de Madrid, 28040 Madrid, Spain

Received June 25, 2005. Revised Manuscript Received August 25, 2005

SiO_2-aerogel inverse opals were produced for the first time in supercritical carbon dioxide ($scCO_2$) with three-dimensional (3D) latex arrays as templates. The polymeric templates were reacted with tetraethyl orthosilicate in humidified $scCO_2$ at 40 °C and 85 bar. After calcination of the template, highly porous materials replicating the structure of the original template were obtained. Polystyrene latex particles decorated with different hydrophilic groups were organized in 3D ordered arrays and used as templates. Particles were impregnated with benzenesulfonic acid, which activates the condensation process of silica precursors. Scanning and transmission electron microscopy (SEM and TEM) images showed that the reaction in $scCO_2$ takes place only on the particle surface and that the octahedral and tetrahedral holes in the original fcc packing of latex spheres are empty. N_2 adsorption isotherms showed broad adsorption−desorption loops characteristic of mesopores. Brunauer−Emmett−Teller (BET) surface areas are large and range from 270 to 594 m^2/g, since these materials are structured aerogels produced directly in $scCO_2$. Analysis of the desorption branch revealed the presence of an extremely large mesoporosity that is located in the macropore walls. The porosity of the materials obtained for each template is different. Furthermore, shrinkage of the network upon condensation in $scCO_2$ was small. The synthesis of inverse opals in $scCO_2$ overcomes some of the limitations of the liquid-phase techniques, being a faster method of synthesis and, at the same time, rendering materials of unique properties.

Introduction

Porous ceramic materials are utilized in catalysis, chromatography, separation, biomaterials, microelectronics, and photonic materials.[1,2] Many of these applications demand materials with controlled pore size and arrangement. The pore size depends on the specific application and ranges from micropores (<2 nm) to mesopores (between 2 and 50 nm) and larger macropores (>50 nm). A very successful way of designing controlled morphologies consists of using a template to direct the synthesis of the ceramic material. After the reaction, the template is removed and the material becomes porous. The smaller pores can be obtained by use of single molecules or small cations as templates (micropores). Larger pores are obtained by use of assemblies of molecules, such as amphiphiles−surfactants and block copolymers (for mesopores). Even larger pores are obtained when polymer spheres or colloidal particles are used as templates (for macropores).[2]

Recently, the synthesis of ordered macroporous materials has received much attention because of their potential use as photonic band gap materials.[3] These new materials must accomplish two important requirements: they must have highly ordered porosity with correlation lengths in the same range as the light wavelength, and they must have a high refractive index contrast. A convenient route to prepare these materials is by the colloidal crystal templating method. SiO_2 or polymer spheres (latex) of particle size in the range of the light wavelength are colloids currently employed. Monodisperse colloidal spheres can be organized in 3D ordered arrays, so-called colloidal crystals, by gravity sedimentation, solvent evaporation, membrane filtration, or centrifugation.[4] These materials are often called opals because they show beautiful colors similar to natural opals. The color changes with the view angle (opalescence) because of the periodic spatial arrangement of the refractive index. To produce the inverse opals, different approaches must be followed according to the opal filler. A suitable precursor is reacted over the colloidal crystal template by sol−gel chemistry, salt precipitation and chemical conversion, chemical vapor deposition, spraying techniques, nanocrystal deposition and sintering, reduction of metal oxides and salts, electrodeposition, or electroless deposition.[4] These methods have been used to produce inorganic oxides, carbons, metals, and polymers.[1,3,5−7] Many of these methods, especially those

* Address correspondence to this author at Departamento de Química-Física I, Universidad Complutense de Madrid, Ciudad Universitaria s/n, 28040 Madrid, Spain. Phone 34 + 91 3944200; fax 34 + 91 3944135; e-mail a.cabanas@quim.ucm.es.

† Departamento de Química−Física I.

‡ Departamento de Química Inorgánica I.

(1) Velev, O. D.; Jede, T. A.; Lobo, R. F.; Lenhoff, A. M. *Nature* **1997**, *289*, 447−448.

(2) Polarz, S.; Smarsly, B. *J. Nanosci. Nanotechnol.* **2002**, *2*, 581−612.

(3) Xia, Y.; Gates, B.; Yin, Y.; Lu, Y. *Adv. Mater.* **2000**, *12*, 693−713.

(4) Stein, A.; Schroden, R. C. *Curr. Opin. Solid State Mater. Sci.* **2001**, *5*, 553−564.

(5) Qi, K.; Yang, Z.; Wang, L.; Liu, Z.; Zhao, D. *Chin. Sci. Bull.* **2000**, *45*, 992−994.

(6) Carbajo, M. C.; Gomez, A.; Torralvo, M. J.; Enciso, E. *J. Mater. Chem.* **2002**, *12*, 2740−2746.

10.1021/cm051382g CCC: $30.25 © 2005 American Chemical Society
Published on Web 11/01/2005

carried out in the liquid phase, are quite time-consuming (involving multistep synthesis or aging), generate large quantities of polluted aqueous waste streams, and can be very energy-intensive (particularly in the drying steps), rendering them environmentally unfriendly. In a recent paper, we reported for the first time the impregnation and reaction of silicon alkoxides precursors into 3D ordered latex arrays in supercritical carbon dioxide ($scCO_2$).[8] The proposed method overcomes some of the limitations of other techniques, being a faster and more sustainable method of synthesis and, at the same time, rendering materials of unique properties. In comparison to a conventional sol−gel technique, the method presents the advantage that it eliminates the drying step necessary to produce aerogel-type materials. In this paper, we further explore the possibilities of this new technique in the fabrication of ordered porous materials. Although SiO_2 is not a candidate to provide a high refractive index contrast in a photonic crystal, the method can be employed in the synthesis of other materials of higher refractive index such as TiO_2 that we are currently considering.

Supercritical fluids are attracting much attention in the synthesis of ceramic materials. $scCO_2$ is by far the fluid most frequently used because it is cheap, nontoxic, and nonflammable and has relatively low critical temperature and pressure ($T_c = 31$ °C, $P_c = 73.8$ bar).[9] Many ceramic precursors such as metal alkoxides dissolve at moderate pressure and temperature in $scCO_2$.[10] The low viscosity, high diffusivity relative to liquids, and very low surface tension of $scCO_2$ promote infiltration in complex geometries and mitigate mass transfer limitations common to liquid-phase processes. CO_2 is a gas at ambient pressure and is eliminated completely upon depressurization. Compressed gases are also highly soluble in polymers, decreasing the glass transition temperature (T_g) of the polymer.[11] The T_g reduction is a macroscopic indication of the enhancement of polymer diffusivity in $scCO_2$, which can affect the mechanical stability of the template and produce aggregation of the polymer particles. This has been the major problem encountered in the synthesis of inverse opals in $scCO_2$ by use of 3D latex array templates. Therefore, much effort has been directed to overcome this problem by introducing modifications in the template moieties, which would avoid particle aggregation.

Aerogels are conventionally made by sol−gel reactions and are dried by use of supercritical fluids.[12] Other researchers have succeeded in making aerogels directly in supercritical fluids. Loy et al.[13] have produced large surface area silica aerogel monoliths from the reaction of tetramethyl orthosilicate and 1,4-bis(triethoxysilyl)benzene directly in $scCO_2$ at 35−45 °C and 414 bar with 13−36% formic acid. Moner-Girona et al.[14] have used formic acid to catalyze the decomposition of tetraethyl orthosilicate (TEOS) in $scCO_2$ and obtained microparticles of silica aerogels at 40−95 °C and 100−150 bar. A similar method was employed to produce silica aerogel films.[15] Sui et al.[16] have compared the activity of acetic, formic, benzoic and chloroacetic acid in the condensation of TEOS in $scCO_2$.

There are also examples of structured ceramic materials produced in $scCO_2$. Pai et al.[17] have shown the preparation of ordered mesoporous silicates in $scCO_2$ using microphase-separated block copolymers. Mesoporous silicate films were prepared by infusion and selective condensation of silicon alkoxides within the hydrophilic blocks of the polymer at 40−60 °C and 120 bar. Because the catalyst *p*-toluenesulfonic acid was confined to the hydrophilic blocks, TEOS did not react in the bulk fluid phase or in the hydrophobic domains. After removal of the template, mesoporous silicate films replicating the structure of the block copolymer were obtained. Wang et al.[18] have recently produced hollow silica spheres with large mesopore wall structure, by reacting TEOS in a CO_2-in-water emulsion in the presence of block copolymers. Other authors have used inorganic supports. Fukushima and Wakayama and co-workers[19,20] have used carbon fibers to produce ceramic and metallic porous materials in $scCO_2$. Impregnation and reaction of TEOS and titanium tetraisopropoxide on the surface of the carbon fibers was carried out without any catalyst at 120−150 °C and 260 bar in $scCO_2$. After calcination or oxidation of the template, a ceramic material with the structure of the carbon fiber was obtained. Finally, the modification of porous materials has been also performed in $scCO_2$. SiO_2−TiO_2 aerogels were produced by impregnation and reaction of titanium alkoxides within silica aerogels.[21,22] The structure of micro- and mesoporous silica was modified by reaction of TEOS in $scCO_2$.[23]

In this paper we report the synthesis of SiO_2-aerogel inverse opals in $scCO_2$. We further explore the possibilities of this new technique in the fabrication of other ordered porous materials using 3D latex array templates of different sizes and compositions.

Experimental Section

Materials. For the synthesis of the polymeric templates, reagent-grade materials from Sigma−Aldrich and distilled water were used.

(7) Carbajo, M. C.; López, C.; Gomez, A.; Enciso, E.; Torralvo, M. J. *J. Mater. Chem.* **2003**, *13*, 2311−2316.
(8) Cabañas, A.; Enciso, E.; Carbajo, M. C.; Torralvo, M. J.; Pando, C.; Renuncio, J. A. R. *Chem. Commun.* **2005**, 2618−2620.
(9) McHugh, M. A.; Krukonis, V. J. *Supercritical Fluid Extraction: Principles and Practice*; Butterworth: Boston, MA, 1986.
(10) Sphul, O.; Herzog, S.; Gross, J.; Smirnova, I.; Arlt, W. *Ind. Eng. Chem. Res.* **2004**, *43*, 4457−4464.
(11) Tomasko, D. L.; Li, H.; Liu, D.; Han, X.; Wingert, M. J.; Lee, J. L.; Koelling, K. W. *Ind. Eng. Chem. Res.* **2003**, *42*, 6431−6456.
(12) Husing, N.; Shubert, U. *Angew. Chem., Int. Ed.* **1998**, *37*, 22−45.
(13) Loy, D. A.; Russick, E. M.; Yamanaka, S. A.; Baugher, B. M.; Shea, K. J. *Chem. Mater.* **1997**, *9*, 2264−2268.
(14) Moner-Girona, M.; Roig, A.; Molins, E.; Llibre, J. *J. Sol−Gel Sci. Technol.* **2003**, *26*, 645−649.
(15) Moner-Girona, M.; Roig, A.; Benito, M.; Molins, E. *J. Mater. Chem.* **2003**, *13*, 2066−2068.
(16) Sui, R.; Rizkalla, A. S.; Charpentier, P. A. *J. Phys. Chem. B* **2004**, *108*, 11886−11892.
(17) Pai, R. A.; Humayun, R.; Schulberg, M. T.; Sengupta, A.; Sun, J.-N.; Watkins, J. J. *Science* **2004**, *303*, 507−510.
(18) Wang, J.; Xia, Y.; Wang, W.; Mokaya, R.; Poliakoff, M. *Chem. Commun.* **2005**, 210−211.
(19) Wakayama, H.; Itahara, H.; Tatsuda, N.; Inagaki, S.; Fukushima, Y. *Chem. Mater.* **2001**, *13*, 2392−2396.
(20) Wakayama, H.; Fukushima, Y. *Ind. Eng. Chem. Res.* **2000**, *39*, 4641−4645.
(21) Yoda, S.; Ohtake, K.; Takebayashi, Y.; Sugeta, Y.; Sako, T. *J. Sol.−Gel. Sci. Technol.* **2000**, *19*, 719−723.
(22) Yoda, S.; Ohtake, K.; Takebayashi, Y.; Sugeta, Y.; Sako, T. *J. Non-Cryst. Solids* **2001**, *285*, 8−12.
(23) Wakayama, H.; Goto, Y.; Fukushima, Y. *Phys. Chem. Chem. Phys.* **2003**, *5*, 3784−3788.

Tetraethyl orthosilicate (99+%) and benzenesulfonic acid (99+%) were obtained from Aldrich. CO_2 (purity >99.99%) was supplied by Air liquid. All chemicals were used as received.

Template Preparation. Monodisperse polystyrene (PS) latex particles microspheres decorated with different hydrophilic groups on their surface were used as templates in the synthesis of macroporous SiO_2. Latex particles were copolymerized in a surfactant-free emulsion in water following a procedure previously described.[6,7,24] The molar ratios of styrene (S) to the monomers methacrylic acid (MA), acrylic acid (AA), and itaconic acid (IA) were 17:1 (PS−MA), 14:1 (PS−AA), and 17:1 (PS−IA). Copolymerization of PS with a mixture of MA and IA (PS−IA−MA) with molar ratios 50:1:2 was also carried out. Suspensions were dialyzed for 4 weeks against water to eliminate residual monomers. Afterward a small amount of benzenesulfonic acid was added to the suspensions, and 3D latex arrays were prepared by centrifugation. Templates were dried under air at room temperature and at 45 °C in an oven. Materials appeared iridescent to the visible light reflecting the 3D ordering of the templates.

Preparation of Macroporous SiO_2 in $scCO_2$. The experiments were conducted in a ca. 70 mL custom-made stainless steel high-pressure reactor in the batch mode. The reactor was loaded with three glass vials each containing (1) pieces of 3D latex arrays (1−5 mm thick), (2) TEOS, and (3) H_2O. Liquid reactants were used in large excess. The reactor was immersed in a thermostatic bath (PolyScience) and filled with CO_2 by use of a high-pressure syringe pump (Isco, Inc. Model 260D) at 40 °C and 85 bar. The pressure was measured with a pressure transducer (Druck Ltd.). A safety valve (Swagelok) was fitted to the reactor. Reaction time varied from 2 to 18 h, although most experiments were conducted for 2 h. Afterward, the reactor was slowly depressurized through a needle valve, in 1−2 h.

At the reaction conditions employed (temperature, pressure, acid concentration, and reaction time), TEOS did not react in the gas phase and condensation took place only on the template. The location of the acid adsorbed to the particle surface and its activity determine the spatial distribution of the condensed SiO_2. When a large excess of TEOS was employed, some TEOS remained in the initial recipient. Upon depressurization, the unreacted TEOS and other reaction byproducts such as EtOH dissolved in the supercritical fluid were vented from the reactor. No additional washing or extraction steps were involved in the experiments described, so during depressurization some TEOS may have precipitated on the template.

Reacted membranes were removed from the reactor and calcined *in air* at 500 °C for 3 h to produce the inverse opals. Temperature was increased from room temperature to 300 °C at 0.5 °C/min and from 300 to 500 °C at 1 °C/min. The weight percentage remaining after calcination was determined by weight difference.

Treatment of the Templates in Pure CO_2. Before the condensation experiments were conducted, the stability of the polymeric templates in pure $scCO_2$ was studied. Pieces of 3D latex arrays of variable thickness were treated in the high-pressure reactor in pure CO_2 under different temperature and pressure conditions. Samples were treated at 30−60 °C and 80−120 bar for a variable period of time from 15 min to 4 h.

Characterization Techniques. Materials were characterized by scanning electron microscopy (SEM), transmission electron microscopy (TEM), Fourier transform infrared spectroscopy (FTIR), and N_2 adsorption experiments. SEM images were taken on a JEOL-6400 electron microscope working at 20 kV. Samples were gold-coated prior to analysis. TEM were carried out on a JEOL 2000FX electron microscope operating at 200 kV equipped with double tilting (±45°) and a JEOL-JEM 3000F electron microscope operating at 300 kV equipped with double tilting (±25°). Samples were dispersed in water or 1-butanol over copper grids and dried in air. FTIR spectra of the powdered materials were recorded as KBr pellets on an IR Prestige-2 spectrometer. N_2 adsorption−desorption isotherms at 77 K were obtained on ASAP-2020 equipment from Micrometrics. Prior to adsorption measurements, samples were outgassed at 110 °C for 2 h. Isotherms were analyzed by the BET equation. Pore size distributions were calculated by the Barrett−Joyner−Halenda (BJH) method for a cylindrical pore model.[25]

Results and Discussion

Treatment of the Templates in CO_2. The large solubility of $scCO_2$ in many polymers has been the subject of numerous studies.[11] The sorption of the fluid in the polymer increases the free volume and segment mobility of the polymer. Macroscopically this translates into a reduction of the polymer glass transition temperature (T_g). The implications of these phenomena are crucial in applications such as polymer separation and fraction, extraction of additives and impurities, drug impregnation, gas separation membranes, production of microparticles, foams, gels, and fibers, and polymerization reactions in $scCO_2$. In the present case, the decrease of the template T_g in $scCO_2$ can affect the ordering and aggregation of the polymeric template. For these reasons, the stability of the 3D latex arrays in $scCO_2$ was studied.

Condo and Johnston[26] have measured T_g of PS as a function of CO_2 pressure by creep compliance. Their data are in agreement with previous data reported by Wissinger and Paulatis.[27] T_g depression of PS is close to 1 °C/bar up to 60 bar and reaches 55 °C at this pressure. A further 10 bar increase of pressure up to 70 bar causes T_g to decrease up to 32 °C. At this temperature T_g becomes pressure-independent up to 110 bar.[26] The sorption of CO_2 in PS at 40 °C and 85 bar is 12−13 wt %.[28] There is much less information about the behavior of the other homopolymers in $scCO_2$ relevant to this study. Kazarian et al.[29] have shown by IR spectroscopy that polymers possessing electron-donating functional groups (e.g., carbonyl groups) such as poly(methyl methacrylate) exhibit Lewis acid−base specific interactions with CO_2. For this polymer, T_g presents retrograde behavior in CO_2 with a maximum pressure at 60 bar.[27,30] Above this pressure, the polymer undergoes plastic deformation. On the contrary, there is evidence suggesting that polymers with carboxylic acid groups are more resistant to CO_2 and can prevent particle aggregation. For example, T_g of poly(acrylic acid) in CO_2 at 80 bar, determined by a chromatographic technique, is 48 °C.[31] Matsuyama et al.[32] have also shown that MA groups act as stabilizers in the

(24) Carbajo, M. C.; Climent, E.; Enciso, E.; Torralvo, M. J. *J. Colloid Interface Sci.* **2005**, *284*, 639−645.
(25) Barret, E.; Joyner, L. G.; Halenda, P. P. *J. Am. Chem. Soc.* **1951**, *73*, 373.
(26) Condo, P. D.; Johnston, K. P. *Macromolecules* **1992**, *25*, 6119−6127.
(27) Wissinger, R. G.; Paulatis, M. E. *J. Polym. Sci., Part B: Polym. Phys.* **1991**, *29*, 631−633.
(28) Aubert, J. *J. Supercrit. Fluids* **1998**, *11*, 163−172.
(29) Kazarian, S. G.; Vincent, M. F.; Bright, F. V.; Liotta, C. L.; Eckert, C. A. *J. Am. Chem. Soc.* **1996**, *118*, 1729−1736.
(30) Condo, P. D.; Johnston, K. P. *Macromolecules* **1992**, *25*, 6730−3732.
(31) KiKic, I.; Vecchione, F.; Alessi, P.; Cortesi, A.; Eva, F. *Ind. Eng. Chem. Res.* **2003**, *42*, 3022−3029.

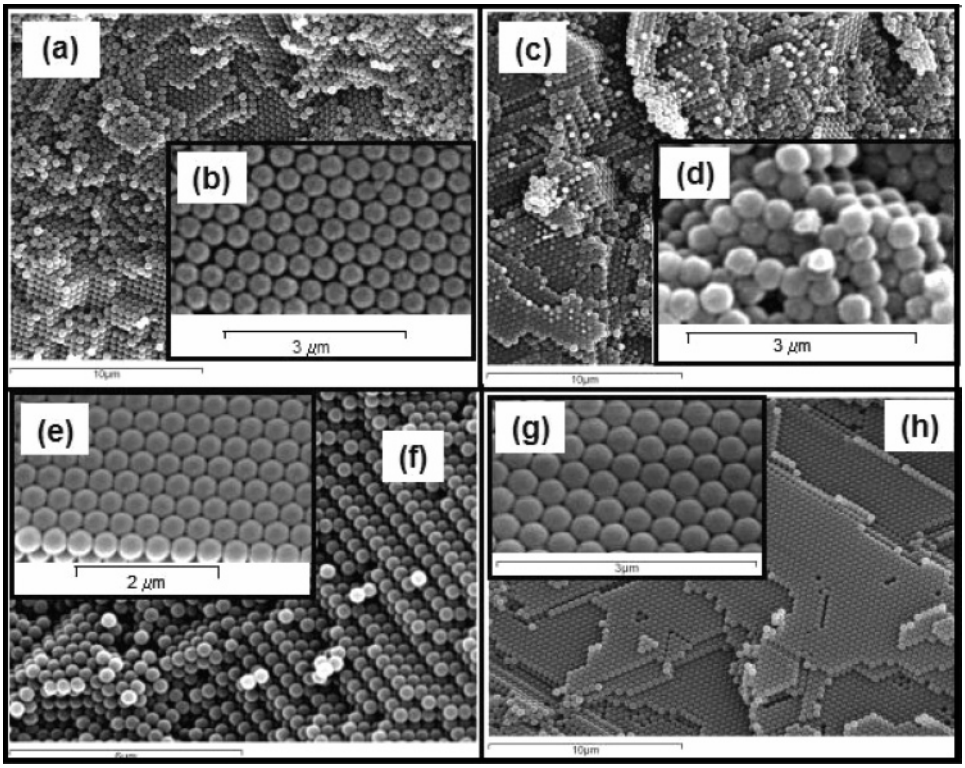

Figure 1. SEM of 3D latex arrays before and after treatment in CO_2 at 40 °C and 85 bar for 2 h: (a, b) PS, (c, d) PS treated in CO_2, (e, f) PS−IA−MA, and (g, h) PS−IA−MA treated in CO_2, Scale bars = (a, c, h) 10 μm, (f) 6 μm, (b, d, g) 3 μm, and (e) 2 μm.

copolymerization of glycidyl methacrylate with MA in $scCO_2$ at 65 °C and 100 bar and were able to produce at these conditions spherical 0.5−5 μm particles. Stabilization of PS particles by the carboxylic acid groups can be electrostatic, electrosteric, or steric in nature. On the other hand, cross-linked PS microspheres can be produced by unstabilized suspension polymerization in $scCO_2$ without surfactants. In this case particles are stabilized against coagulation by their rigid, cross-linked surfaces.[33]

Three-dimensional latex arrays of particles with sizes between 150 and 550 nm were treated in CO_2 under different temperature and pressure conditions and studied by SEM. A series of experiments was conducted at 50 °C and 85 bar for 15−60 min and have been reported elsewhere.[34] Although these conditions are above the glass transition of PS in CO_2,[26] particle aggregation showed a clear dependence on the particle composition. Particle aggregation in PS−AA and PS−MA 3D latex arrays as determined by SEM was much weaker than in bare PS. PS−IA particles did not aggregate at these conditions, although 3D order was lost. A similar effect was found when cross-linked PS particles were treated in CO_2.

Further experiments were conducted at 40 °C and 85 bar for 2 h (also above the glass transition of pure PS under these conditions). Figure 1 shows SEM pictures of a PS 3D latex array composed of 400 nm particles before (a, b) and after the treatment in CO_2 (c, d). Significant aggregation of the particles treated in CO_2 under these conditions can be observed. On the contrary, SEM analysis of PS−MA, PS−IA, and PS−IA−MA showed that particles do not aggregate significantly at the same conditions. SEM pictures of a PS−IA−MA 3D latex array composed of 350 nm particles before (e, f) and after the treatment in CO_2 (g, h) show that CO_2 does not seem to affect the morphology of the polymeric template. A detailed study of the particle aggregation and stabilization process is underway.

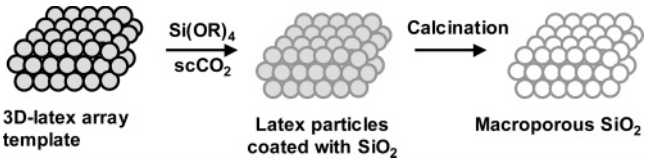

Figure 2. Preparation of macroporous SiO_2 in $scCO_2$.

Preparation of Macroporous SiO_2 in $scCO_2$. A schematic representation of the process followed in the preparation of periodic macroporous SiO_2 is illustrated in Figure 2. A 3D latex array template with adsorbed acid at the surface is reacted with a silicon alkoxide precursor [$Si(OR)_4$] dissolved in $scCO_2$. After the reaction, the material is calcined and the polymeric template is removed.

Decomposition of $Si(OR)_4$ compounds has been carried out in $scCO_2$.[13−17] The process seems to proceed through the traditional sol−gel steps: (i) hydrolysis, $Si(OR)_4 + H_2O \rightarrow Si(OR)_3{-}OH + R{-}OH$, and (ii) condensation, $(OR)_xSi{-}OH + XO{-}Si(OR)_y \rightarrow (OR)_xSi{-}O{-}Si(OR)_y + XOH$, where X = R, H. When the reaction is carried out in $scCO_2$, the alcohol generated from the hydrolysis and condensation reactions (R−OH) dissolves in the reaction medium, thus

(32) Matsuyama, K.; Mishima, K.; Takahashi, K.; Ohdate, R.; Tomokage, H. *J. Chem. Eng. Jpn.* **2003**, *36*, 516−521.
(33) Cooper, A. I.; Hems, W. P.; Holmes, A. B. *Macromol. Rapid Commun.* **1998**, *19*, 353−357.
(34) Cabañas, A.; Enciso, E.; Carbajo, M. C.; Torralvo, M. J.; Pando, C.; Renuncio, J. A. R. In *6th International Symposium on Supercritical Fluids*; International Society for the Advancement of Supercritical Fluids; Trieste, Italy, 2004; CD-ROM.

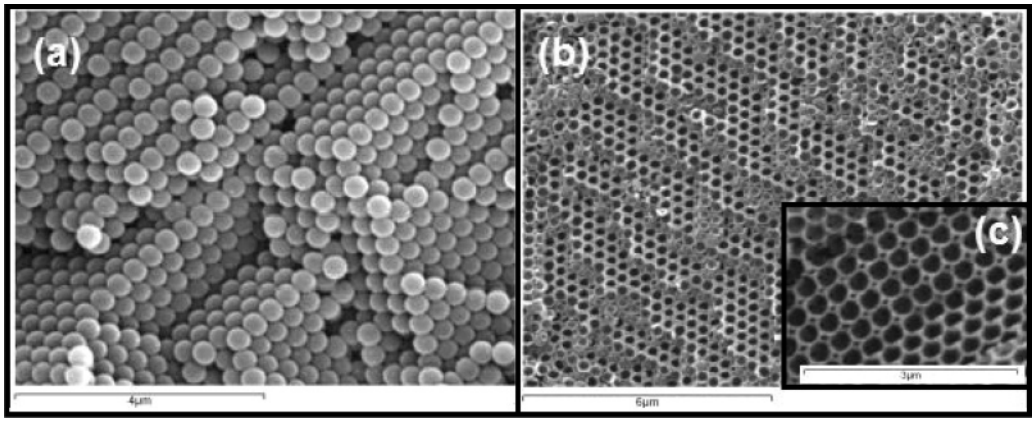

Figure 3. SEM of a PS−IA−MA 3D latex array used as template (a) and the periodic macroporous SiO_2 obtained after reaction of TEOS in $scCO_2$ (b, c). Scale bars = (a) 4 μm, (b) 6 μm, and (c) 3 μm.

driving hydrolysis and condensation reactions toward products.[35]

The decomposition of TEOS in $scCO_2$ can be carried out at 120 °C without any catalyst.[19,20] When an acid catalyst such as formic acid is used, however, the reaction temperature can be as low as 35 °C.[13] Sui et al.[16] have studied the catalytic decomposition of TEOS and shown that the reaction rate clearly increases with temperature but decreases if the CO_2 pressure is increased. The higher reaction rates at lower pressure are explained as a consequence of the preferential clustering. Condensation seems to rise remarkably by the addition of a small amount of water.

In this work, due to the limited stability of the polymeric templates, the reaction temperature was maintained low. Organic acids attached to the particle surface catalyzed the precursor decomposition. Pressure was kept high enough to dissolve a sufficient amount of precursor. Catalytic decomposition of TEOS in humidified $scCO_2$ was carried out at 40 °C and 85 bar on 3D latex particle arrays impregnated with benzenesulfonic acid. After reaction, the template was removed by calcination and light-blue colored powders were obtained. SiO_2 loading after calcination represented 3−7 wt % with respect to the composite material. Since the density of silica in the materials produced in $scCO_2$ is unknown, it is not possible to evaluate the yield of the process from this figure. In controlled conditions, however, the fraction of nontemplated SiO_2 observed by SEM is very low. Calcination of the reacted templates renders powders instead of monoliths, probably because of the existence of defects in the original template.

FTIR spectra of the polymeric templates showed bands ascribed to the corresponding homopolymers. The membranes impregnated with benzenesulfonic acid showed a very weak band due to the sulfonic acid group at 1128 cm^{-1} (the amount of catalyst required was very small). FTIR spectra of the samples infused and reacted in $scCO_2$ showed broad and intense Si−O−Si bands (1000−1250 cm^{-1}) superimposed on those of the template. After calcination, only Si−O−Si bands were observed. The Si−O−Si bands shifted to higher wavenumbers after calcination, thus suggesting the strengthening of the Si−O bond.

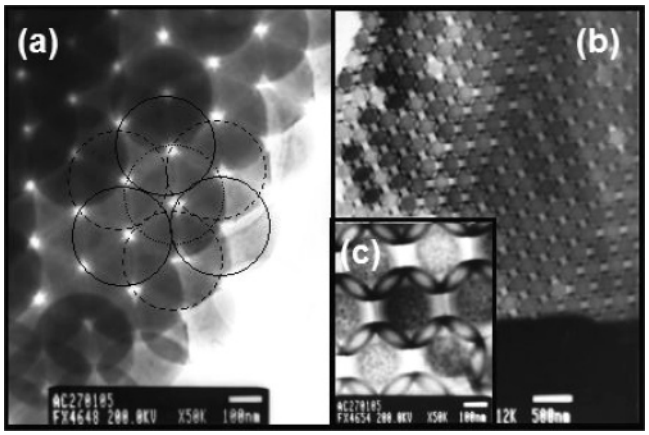

Figure 4. TEM of the composite material obtained after infusion of TEOS in $scCO_2$ on a PS−IA−MA template (shown in Figure 3) along the [111] (a) and [110] (b, c) directions. Scale bars = (a) 100 nm, (b) 500 nm, and (c) 100 nm.

Figure 3 shows SEM pictures of a PS−IA−MA template impregnated with 0.01 M benzenesulfonic acid (a) and the macroporous SiO_2 obtained after reaction of TEOS in $scCO_2$ (b and c). The material was reacted in $scCO_2$ at 40 °C and 85 bar for 4 h and further calcined at 500 °C for 3 h. The PS−IA−MA template is composed of monosized 350 nm round particles self-organized in 3D ordered arrays. The template presents regions of fcc packing together with some less ordered regions. SEM images of the inverse opal reveal an ordered macroporous material, which replicates the structure of the original template. SEM shows holes among the hollow spheres as well as seams between adjacent spheres, which suggests that the reaction of the precursor at these conditions takes place only at the particle surface.

The ordering of the voids in the material is better observed by TEM. Figures 4 and 5 show TEM pictures of the reacted template before and after calcination, respectively, along the [111] and [110] projections. Images reveal that after reaction in $scCO_2$, the ordering of the template is preserved. The layers A, B and C of the fcc packing have been drawn in the projections [111] (Figures 4a and 5a). TEM images prove that the reaction occurs only on the particle surface and that both tetrahedral and octahedral holes in the structure are empty. Figures 4b,c and 5b−e show projections along the

(35) Ziegler, J. M.; Chester, T. L.; Innis, D. P.; Page, S. H.; Dorsey, J. G. In *Innovations in Supercritical Fluids*; Hutchinson, K. W., Foster, N. R., Eds.; American Chemical Society: Washington, DC, 1996; Vol. 608, pp 93−110.

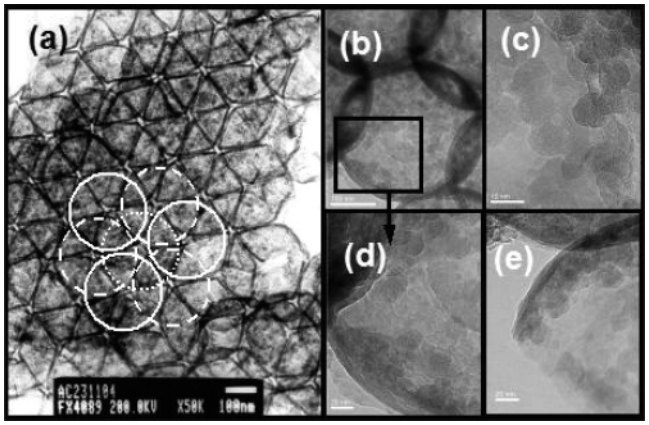

Figure 5. TEM of a periodic macroporous SiO_2 obtained after infusion of TEOS in $scCO_2$ on a PS−IA−MA template and calcination, along the [111] (a) and [110] (b−e) directions. Scale bars = (a, b) 100 nm, (c) 10 nm, and (d, e) 20 nm.

[110] direction. Figure 4b of the composite material before calcination shows several twins in the 3D crystal. The inset in the figure (Figure 4c) shows a higher magnification image of the same projection. The particle surface of the composite material has a granular appearance. The discrete darker regions may indicate discontinuous deposits of silica where condensation occurs and suggest a large porosity in the wall. The same can be observed in Figure 5b−e, which show higher magnification TEM images of the same sample after calcination along the [110] direction. These pictures show walls formed by 5−10 nm grains. SEM and TEM pictures clearly indicate that the reaction in $scCO_2$ happens only at the particle surface.

For comparative purposes, a piece of PS−IA−MA 3D latex array impregnated with 0.2 M benzenesulfonic acid was infused by capillarity with a solution of TEOS/H_2O/EtOH of molar ratio 1:4:4.5. A ratio of TEOS:H_2O equal to 1:4 was considered optimum for complete hydrolysis of the precursor (without taking into account the water generated from condensation). EtOH was required to maintain TEOS and H_2O in one phase. After 18 h the sample was calcined at 500 °C for 3 h and studied by the same experimental techniques. Figure 6 shows TEM pictures of the material produced by the sol−gel reaction in the liquid medium along the [111] direction and a projection close to the [100] direction. As in previous figures, the layers A, B, and C of the fcc packing have been drawn in the [111] projection. Although the infusion in the liquid phase has not been optimized, TEM pictures show that the reaction proceeds by filling the tetrahedral and octahedral holes and that there is no space between voids.

Another difference between the materials obtained from reactions in the liquid and supercritical media is the shrinkage of the network. The size of the original PS−IA−MA latex particles is close to 350 nm. After infusion with TEOS in $scCO_2$, SiO_2 coated particles showed a slight shrinkage, with a particle size close to 330 nm by TEM (Figure 4). After removal of the template by calcination, the distance between pore centers determined by SEM and TEM (Figures 3b and 5) was further reduced to 300 nm, which represents 14% shrinkage with respect to the original particle size. In contrast, the shrinkage of the network when the reaction is performed

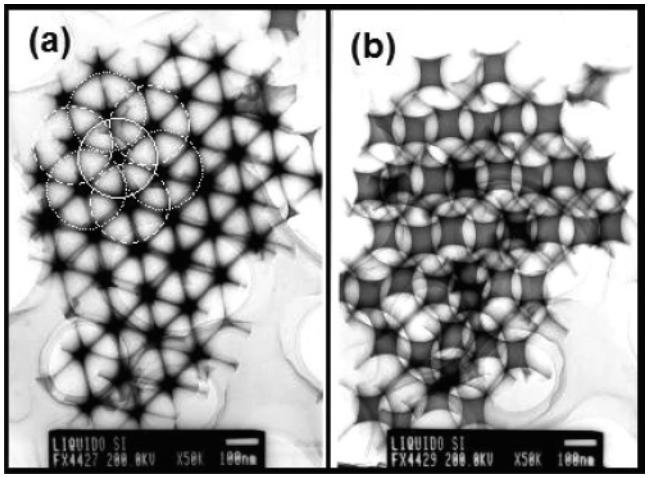

Figure 6. TEM of a periodic macroporous SiO_2 obtained by infusion of a TEOS/H_2O/EtOH solution on a PS−IA−MA template after calcination along the [111] direction (a) and a projection close to the [100] direction (b). Scale bars = 100 nm.

in the liquid phase is close to 24% (Figure 6). The smaller shrinkage observed when the reaction is performed in $scCO_2$ is related to the high solubility of ethanol in the solvent.[35] The elimination of alcohol excess from the reaction media provides a pathway for a rapid and substantial network condensation and minimal shrinkage during template removal. Although the shrinkage of the network after particle coating in $scCO_2$ is very small, small seams between adjacent spheres appear after calcination (Figure 5a).

Other authors have also reported large shrinkages when the infusion is carried out in the liquid phase. Holland et al.[36] produced SiO_2 inverse opals by using PS latex spheres of size 420−700 nm and liquid TEOS solutions. Liquid mixtures of TEOS and EtOH of different ratios were infused into the 3D latex arrays. After calcination of the template, 26−34% shrinkage of the structure was reported. Carbajo et al.[7] have found a similar shrinkage, ca. 22%, when 3D arrays of 260 nm PS particles were infused with sodium silicate solutions.

To further prove the capabilities of our method, we have produced macroporous SiO_2 using other 3D latex array templates of different sizes and compositions. Using 3D latex arrays of PS−MA particles, 170 nm size, previously impregnated with 0.007 M benzenesulfonic acid, we have produced SiO_2 membranes with a distance between macropores equal to 140 nm. Shrinkage in this case is larger, 18%. Figure 7 shows SEM pictures of the template (panel b) and the macroporous material obtained after reaction of TEOS in $scCO_2$ at 40 °C and 85 bar and calcination (panels a and c). The inverse opal replicates the structure of the template.

We have also produced larger macroporous materials using 3D latex arrays of PS−IA particles impregnated with 0.01 M benzenesulfonic acid, 530 nm size. Figure 7 shows SEM pictures of the PS−IA template (panel e) and the inverse opal obtained from condensation of TEOS at 40 °C and 85 bar (panels d and f). Figure 7f shows a region where macropores appear interconnected by windows. Figure 8 shows TEM projections of this sample along the [111] and

(36) Holland, B. T.; Blanford, C. F.; Do, T.; Stein, A. *Chem. Mater.* **1999**, *11*, 795−805.

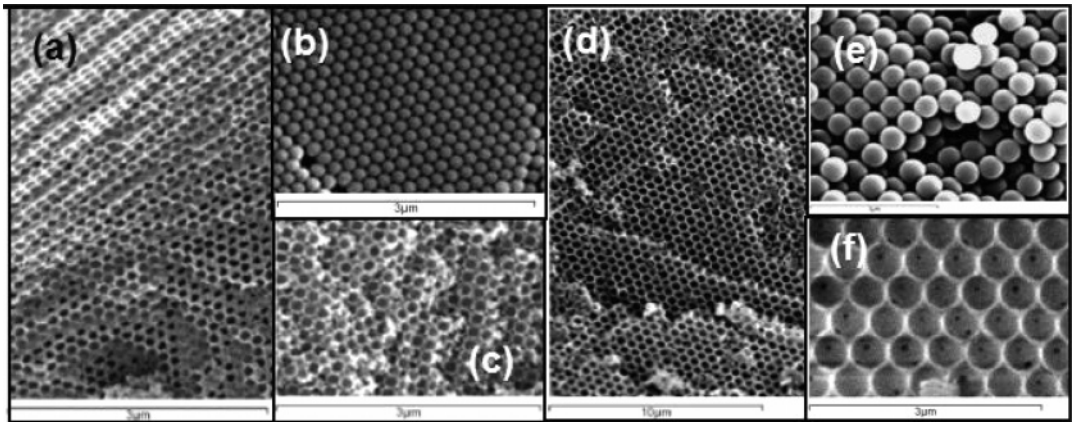

Figure 7. SEM of PS−MA and PS−IA 3D latex arrays used as templates (b and e, respectively) and the periodic macroporous SiO_2 obtained after reaction of TEOS in $scCO_2$ and calcination for PS−MA (a and c) and PS−IA (d and f). Scale bars = (a−c, e, f) 3 μm and (d) 10 μm.

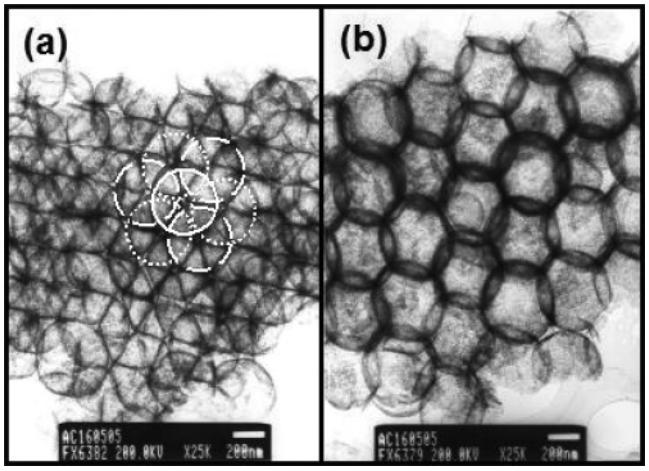

Figure 8. TEM of a periodic macroporous SiO_2 obtained after infusion of TEOS in $scCO_2$ on a PS−IA template after calcination, along the [111] (a) and [110] (b) directions. Scale bars = 200 nm.

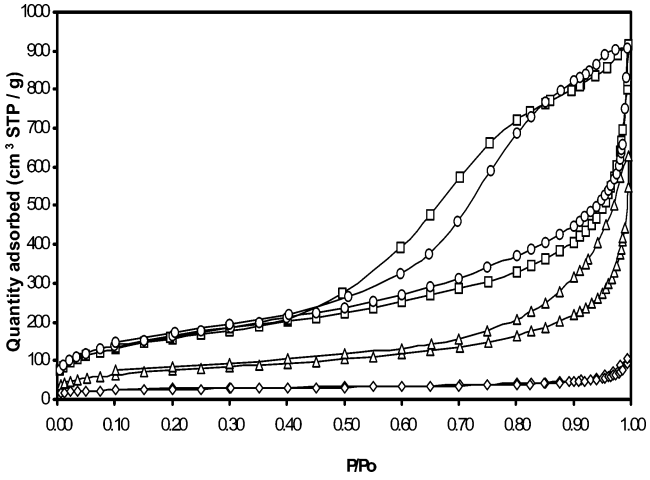

Figure 9. Adsorption−desorption isotherms of macroporous SiO_2 produced by the reaction of TEOS in $scCO_2$ with (□) PS−IA−MA, (○) PS−MA, and (△) PS−IA templates and by the reaction of TEOS in the liquid medium with (◇) PS−IA−MA template.

[110] directions. TEM of this material confirmed that the reaction takes place only on the particle surface. After reaction, the pore distance becomes 490 nm; thus shrinkage of the network represents only 8% of the size of the original template. However, as in the previous examples, small seams between particle voids are observed in the [111] projection. TEM images show voids less spherical than those obtained with the PS−IA−MA template. Wall thickness in this case seems to be slightly thinner.

The previous experiments show that the particle composition affects the condensation reaction. In particular, reactivity seems to increase with MA content in the template (PS−MA > PS−IA−MA > PS−IA). Materials obtained with the PS−MA template yielded thicker wall materials and experienced a larger shrinkage of the network upon condensation. In contrast, materials produced with the PS−IA template showed thinner walls and a much lower shrinkage. In this case, the appearance of regions where macropores are interconnected by windows is related to the lower reactivity of the PS−IA template. PS−IA−MA exhibited a behavior closer to PS−MA.

The method outlined in Figure 2 is general, as long as the template withstands the CO_2 treatment and the catalysts adsorbs to the particle surface. The adsorption of the catalyst seems to be crucial in determining the success of the process, and large variations with the catalyst concentration and the particle composition have been found. If the catalyst concentration is too large, excess SiO_2 deposits quickly on the template, blocking the pore system and preventing further penetration of the precursor. Therefore for high catalyst concentrations, a very low yield is obtained. On the other hand, if the catalyst concentration is too low, for opposite reasons, the yield after calcination is also very low. An optimal concentration of the catalyst has been identified for these conditions.

Gas Adsorption. N_2 adsorption experiments confirmed the unique porosity of the materials produced in $scCO_2$. In all cases type IV adsorption isotherms in the IUPAC classification were obtained.[37] All samples showed hysteresis with a broad adsorption−desorption loop intermediate between types H2 and H3. The isotherms of the different materials are shown in Figure 9. Adsorption isotherms for the macroporous SiO_2 obtained from the reaction of TEOS in $scCO_2$ with PS−IA−MA and PS−MA templates showed very broad hysteresis loops. For PS−IA templates, the volume adsorbed was lower and the hysteresis loop was narrower. N_2 adsorption analysis of the material produced by sol−gel reaction in the liquid medium with a PS−IA−

(37) Gregg, S. J.; Sing, K. S. W. *Adsorption, Surface Area and Porosity*, 2nd ed.; Academic Press Inc.: London, 1982.

Table 1. Characteristic Parameters of the Different Materials

template	medium	latex particle size (nm)	void size[a] (nm)	shrinkage (%)	S_{BET} (m^2/g)	S_{geo} (m^2/g)
PS−IA−MA	CO_2	350	300	14	570	38
PS−IA−MA	liquid	350	265	24	92	22
PS−MA	CO_2	170	140	18	594	82
PS−IA	CO_2	530	490	8	270	23

[a] Distance between pore centers estimated from SEM and TEM.

MA template also showed a type IV isotherm with a much smaller hysteresis loop.

Table 1 summarizes surface area obtained for the different materials by use of the BET model (S_{BET}). The maximum geometrical area (S_{geo}) was calculated as the sum of the internal and external surface of the silica hollow spheres (estimated as twice the surface generated by the voids, for a void size given). Table 1 also presents the percent shrinkage of the network after condensation observed in the different examples studied.

The volume adsorbed in every sample was compared to a nonporous silica standard (LiChrospher Si-1000)[38] in reduced units (divided by the adsorbed volume at a reduced pressure P/P_0 equal to 0.4). Comparison of the adsorption data for the materials produced in $scCO_2$ showed almost complete overlapping with the standard in the low-pressure range before gas condensation, which indicates the absence of microporosity in the samples. At higher relative pressures, adsorption of the samples produced in CO_2 showed positive deviations from the standard. The sample produced in the liquid phase, however, showed completely different behavior, with enhanced adsorption at low pressure and larger deviations with respect to the reference. At higher pressures, adsorption isotherm of the material produced in the liquid phase laid under the standard. By use of the α_s plot method[37] a micropore volume of 0.009 cm^3/g was obtained for the sample produced in the liquid medium. For the materials produced in $scCO_2$, in all cases values very close to zero were found from the fit.

S_{BET} in the experiments carried out in $scCO_2$ are very large and range from 270 m^2/g for the material templated with PS−IA to 570 and 594 m^2/g for those materials templated with PS−IA−MA and PS−IA, respectively. S_{geo} is very small compared to S_{BET} and therefore, in the absence of micropores, the major contribution to the area is due to the mesopores. The proposed method yields structured aerogel materials templated by the 3D latex arrays. The surface composition of the template affects the surface area of the inverse opal material.

Similar high surface area materials have been obtained in other experiments performed in $scCO_2$. For example, SiO_2 samples obtained from sol−gel reactions performed directly in $scCO_2$ showed surface areas of 260−586 m^2/g in the case of monoliths[13] and 400−600 m^2/g for aerogel microparticles.[14] Furthermore, analysis of the porosity of mesoporous silicate films prepared by infusion and selective condensation of silicon alkoxides within the hydrophilic blocks of a microphase-separated block copolymer in CO_2 have also revealed an extremely high micropore volume, generated by the interpenetrating networklike structure with the silicate network during infusion and condensation of the precursor.[39]

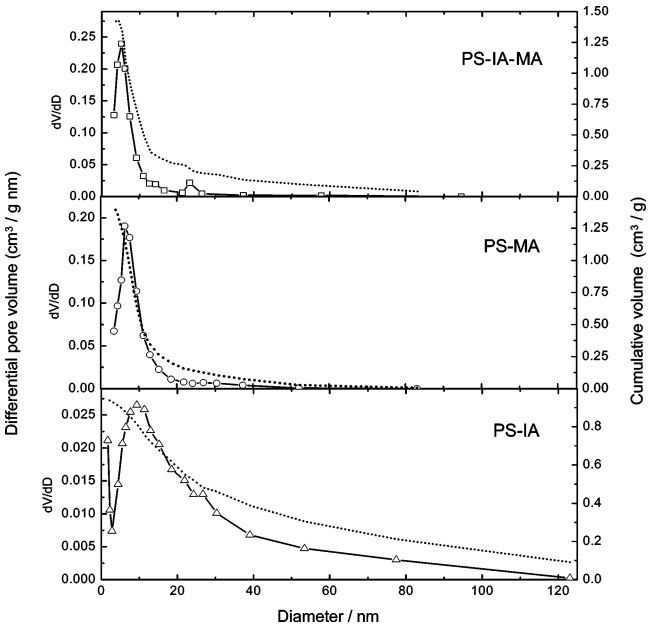

Figure 10. Size distribution obtained from the desorption branch of the isotherms for macroporous SiO_2 produced by reaction of TEOS in $scCO_2$ with (□) PS−IA−MA, (○) PS−MA, and (△) PS−IA templates. Cumulative volumes are shown as dotted lines on each graph.

In contrast, S_{BET} of the material synthesized in this work in the liquid medium was only 92 m^2/g. Other authors have reported S_{BET} between 173 and 231 m^2/g for SiO_2 inverse opals prepared from the condensation of TEOS and EtOH liquid mixtures.[36] These higher values, however, are still much lower than those found in the samples produced in $scCO_2$. The materials produced in $scCO_2$ are aerogels of large surface area, while the materials produced by sol−gel reactions in a liquid phase and air-dried are xerogels of lower surface area.[40]

The adsorption isotherms were studied by the BJH method[25] for a cylindrical pore model. Analysis of the adsorption branch gave a monotonically decreasing pore size distribution from the lowest mesopores to 150 nm without special features. Analysis of the desorption branch was more informative, and sharp size distributions with maxima in the mesopore range were obtained. Size distributions calculated from the desorption branch are presented in Figure 10 along with the cumulative adsorbed volume. The material templated with PS−IA−MA showed a maximum at ca. 5 nm along with other weaker relative maxima between 20 and 30 nm. The material templated with PS−MA presented a size

(38) Jaroniec, M.; Kruk, M.; Olivier, J. P. *Langmuir* **1999**, *15*, 5410−5413.

(39) Vogt, B. D.; Pai, R. A.; Lee, H.-J.; Hedden, R. C.; Soles, C. L.; Wu, W.-L.; Lin, E. K.; Bauer, B. J.; Watkins, J. J. *Chem. Mater.* **2005**, *17*, 1398−1408.

(40) Brinker, C. J.; Scherer, G. W. *Sol−gel science: The physics and chemistry of sol−gel processing*; Academic Press: Boston, MA, 1990.

distribution very similar to the previous one, with a maximum at ca. 6 nm. The material templated with PS−IA, however, showed a much broader size distribution with a maximum between 8 and 11 nm, which extends considerably up to 40−60 nm with a shoulder at 25−30 nm. Gas adsorption in this case was also lower.

In the materials produced in $scCO_2$, N_2 adsorbs into the walls of the voids left by the template and, at higher pressures, condensation in the tetrahedral and octahedral holes between voids takes place. These features, however, have not been captured by the pore distribution curve obtained from the adsorption branch because the filling of tetrahedral and octahedral holes occurs through the pore walls. For the latex particle sizes used, the voids generated by calcination of the template are too large to be filled with gas at these pressures, as can be inferred from the adsorbed cumulative volumes. The variable pore diameter and the connectivity in the pore system explain the broad pore size distribution obtained from the adsorption branch.[24] Additional information can be obtained from the desorption branch. The evaporation of the gas adsorbed happens through the smallest pores, because they limit the desorption in a multimodal connected porous network. In all the distribution curves, the maximum appears in the mesopore range at 5−10 nm. Inspection of the TEM images of the different materials indicates that these mesopores must be located in the void walls.

The chemical composition of the template affects the hydrolysis and condensation reactions and, as a result, a different porosity is obtained in the different samples. The materials templated with PS−MA and PS−IA−MA exhibit very narrow size distributions with maxima at ca. 5 nm. TEM images of the material templated with PS−IA−MA (Figures 3 and 4) already suggested a large porosity in the walls. In this case the relative maximum between 20 and 30 nm can be related to the window formed by three neighboring hollow spheres. The size distribution for the material templated with PS−MA is very similar to the previous one but it only presents a clear maximum, which suggests a higher loading of ceramic in the sample. Nevertheless, the cumulative volume obtained from the desorption branch at 25−30 nm size is not negligible, supporting the gas sorption in the tetrahedral and octahedral holes. The much broader size distribution obtained for the material templated with PS−IA indicates a less homogeneous pore system and therefore heterogeneity in the void walls. TEM images of this sample (Figure 8) also suggest large porosity in the ceramic walls. The size distribution of the material templated with PS−IA shows a shoulder between 25 and 30 nm, which may be related to the window formed by the neighboring spheres. Since adsorption happens mostly in the ceramic walls, the thinner walls observed by TEM in the PS−IA inverse opal would explain the lower gas adsorption.

Analysis of the adsorption isotherms provides substantial information about the pore wall structure and connectivity of the inverse opals. More efforts must be made in order to improve the theoretical tools of analysis and the structural identification of the main features of the adsorption isotherms and their relationship with the porous morphology.

Conclusions

A new method to produce ordered macroporous ceramic materials by sol−gel reaction of silicon alkoxides in $scCO_2$ by use of 3D latex array templates is presented. The process has been demonstrated for three different latex particles, PS−MA, PS−IA, and PS−IA−MA, of sizes 170, 530, and 350 nm, respectively. These templates have been reacted with TEOS in $scCO_2$ at 40 °C and 85 bar. The inverse opal materials obtained after calcination of the template have been fully characterized. In comparison to the process in the liquid phase, the reaction in $scCO_2$ takes place only on the particle surface. Furthermore, the materials synthesized in $scCO_2$ present a very high surface area, mostly due to mesopores located in the macropore wall. The composition of the template affects the surface reaction, and differences have been observed among the different materials. The inverse opals produced with PS−MA and PS−IA−MA templates present extremely narrow mesopore size distributions. These new hierarchical materials produced in $scCO_2$ can have interesting applications in catalysis. This is a new method to produce structured macroporous aerogels. We are currently studying ways of controlling the porosity of the walls as well as working in the synthesis of other macroporous materials.

Acknowledgment. We gratefully acknowledge the financial support of MCyT (Spain), research projects MAT2002-04540-C05-05 and PPQ2003-04143-C02-02. A.C. thanks MCyT (Spain) for its support through a Ramón y Cajal contract. We also thank the Centro de Microscopía Electrónica at UCM for technical assistance.

CM051382G